Ocean bays surrounded by desert land could support photosynthetic life on Snowball Earth

Greta E.M. Shum[1,2,*], Marysa M. Laguë[3], Abigail L.S. Swann[1,4], Cecilia M. Bitz[1,2], Edwin D. Waddington[5], and Stephen G. Warren[1,2,5]

[1]Department of Atmospheric Sciences, University of Washington, Seattle, WA 98195, USA.

[2]Astrobiology Program, University of Washington Seattle, WA 98195, USA.

[3]Department of Atmospheric Sciences, University of Utah, Salt Lake City, UT 84112, USA.

[4]Department of Biology, University of Washington, Seattle, WA 98195, USA.

[5]Department of Earth and Space Sciences, University of Washington, Seattle, WA 98195, USA.

For submission to *AGU Advances*

21 March 2024.

*Corresponding author. Email: gshum@uw.edu

Key points:

- Snow-free desert land (with albedo lower than the frozen ocean) can warm the local climate.
- Lowering land-surface albedo expands the area of net-sublimating, snow-free land.
- Numerous narrow-bay refugia for photosynthetic life (places with surface temperatures above freezing) can exist on Snowball Earth.

Keywords: Snowball Earth, sea ice, albedo, sea glacier, radiative forcing, refugia

Abstract

Photosynthetic eukaryotic algae survived the Neoproterozoic Snowball Earth events, indicating that liquid-water refugia existed somewhere on the surface. We examine the potential for refugia at the coldest time of a snowball event, before CO_2 had risen and with high-albedo ice on the frozen ocean, before it became darkened by dust deposition. We use the Community Earth System Model to simulate a "modern" Snowball Earth (i.e., with continents in their current configuration), in which the ocean surface has frozen to the equator as "sea glaciers", hundreds of meters thick, flowing like ice shelves. Despite global mean surface temperatures below -60°C, some areas of the land surface reach above-freezing temperatures because they are darker than the ice-covered ocean. With low CO_2 (10 ppm) and land-surface albedo 0.4 (characteristic of bright sand-deserts), 0.1 percent of the land surface could host liquid water seasonally; this increases to 12 percent for darker land of albedo 0.2, characteristic of polar deserts. Narrow bays intruding from the ocean to these locations (such as the modern Red Sea) could provide a water source protected from sea-glacier invasion, where photosynthetic life could survive. The abundance of potential refugia increases more strongly in response to reducing the land albedo than to increasing the CO_2, for the same global radiative forcing.

Plain language summary

Two “Snowball Earth” events occurred approximately 600 million years ago, when the shape and location of continents were different from today. During these events, the ocean was apparently covered with “sea glaciers”, hundreds of meters thick, which flowed like ice shelves. Yet photosynthetic algae survived these events, indicating that small regions of liquid water (“refugia”) existed somewhere on the surface. An Earth System Model shows that, even with global average surface temperature below -60°C, some areas of the land surface reach above-freezing temperatures because they are darker than the ice-covered ocean. Narrow bays intruding from the ocean to these locations (such as the modern Red Sea) could provide a water source protected from sea-glacier invasion, where photosynthetic life could survive.

1. Introduction

On Earth and Earth-like worlds, a large negative radiative forcing can initiate a positive ice-albedo feedback and ultimately lead to global glaciation (Budyko, 1969; Sellers, 1969). Geologic evidence indicates that the Earth has experienced several such events since the emergence of life (Harland, 1964; Kirschvink, 1992; Hoffman et al., 2017; Evans, 2000). These events were likely caused by a reduction of the atmospheric greenhouse effect, resulting from disturbance of the global carbon cycle (Hoffman et al., 2017). During the Neoproterozoic era (600-800 Ma), two "Snowball Earth" events occurred: the Sturtian, with a duration of 58 million years, and the Marinoan, with a duration of ~10 million years (Macdonald et al., 2010). The oceans would likely have been covered by ice hundreds of meters thick, but photosynthetic eukaryotic algae were able to survive (Porter, 2004; Knoll, 2011, 2014), indicating that some liquid water was maintained at or near the surface where light was available for photosynthesis.

In this paper, we focus on the "hard" Snowball Earth, in which the equatorial ocean would be covered by thick ice. That ice differed in several ways from sea ice on the polar oceans of modern Earth. Modern sea-ice thickness is limited to a few meters by summertime melting and by a heat flux F_0 of several watts per square meter from the ocean water below, which originally gained its heat by absorption of solar energy at lower latitudes. But at the onset of a snowball event, when sea ice reached the equator it would shut off solar heating of the ocean water below. After a few thousand years, the ocean would have lost its reservoir of heat, leaving only geothermal heat, $F_0 \approx 0.08$ W m^{-2} (about one-hundredth that of the modern oceanic flux F_0 to the ice bottom), increasing the equilibrium ice thickness from a few meters to a few hundred meters (Warren et al., 2002).

The geothermal flux is essentially independent of latitude, but the ice surface on the snowball ocean would be colder at high latitude than at low latitude, resulting in thicker ice at higher

latitude. The latitudinal thickness gradient would cause the ice to flow (Goodman and Pierrehumbert, 2003). In this state, the thick ice on the frozen ocean would be growing from above by snowfall (the original sea ice having melted off the bottom), and therefore can be classified as glacier ice rather than sea ice. This ice, flowing like the modern Antarctic ice shelves but not dependent on continental glaciation, is called a *sea glacier* (Warren et al., 2002). Sea glaciers are computed to flow as much as 7-50 meters per year even when they cover the entire ocean (Goodman, 2006; Li & Pierrehumbert, 2011). If a small area of the ocean were to open up, it would be quickly filled by inflow of the sea glacier. How, then, could liquid water be maintained at the surface? Several hypotheses for refugia have been proposed, which we now list.

1.1. Types of proposed refugia

Five ideas have been proposed for liquid-water refugia at the ocean surface.

(a) Hotspots. Hoffman and Schrag (2000, 2002) noted that geological hotspots at the ocean floor under shallow water, as occur near the coasts of Hawaii and Iceland, would melt inflowing ice fast enough to maintain pools of liquid seawater. These pools would be small in area, and would not be stable for millions of years, so any life would have to survive many long and deep migrations.

(b) Thin ice. McKay (2000), using a broadband model for solar radiation, proposed that absorption of sunlight within the ice might be able to limit the tropical ice thickness to ~10 m. Warren et al. (2002) pointed out that the visible and ultraviolet wavelengths, which penetrate deeply, are not absorbed but eventually are scattered back out to space, whereas the near-infrared wavelengths, which are indeed absorbed, are absorbed in the top few millimeters, so their heat is easily conducted up to the atmosphere. By modifying McKay's model to compute the radiation

spectrally, Warren et al. found that the equilibrium ice thickness in a typical example grew from 1 m to 800 m. McKay joined as a coauthor on that paper, agreeing that the thin-ice solution was not viable. Pollard and Kasting (2005) tried to find a thin-ice solution that would even hold off sea glaciers, and succeeded only when three parameters were pushed beyond their acceptable limits (Warren and Brandt, 2006). An improved model (Pollard et al., 2017) convincingly rejected the thin-ice solution.

(c) Waterbelt. Some models of snowball initiation have found that sea ice could reach the outer tropics but still leave a wide belt of open water centered on the equator, spanning tens of degrees of latitude and circling the globe, if the sea-ice (or sea-glacier) albedo is low enough. Abbot, Voigt, and Koll (2011) found that this "waterbelt" state could exist with sea-glacier albedo of 0.45 but is inaccessible for sea-glacier albedo >0.55. Dadic et al.'s (2013) measurements of modern surrogates for sea-glacier surfaces found albedos 0.57-0.80 under clear sky, and even higher under cloudy sky, arguing against the waterbelt idea. A follow-on investigation by Voigt's group (Braun et al., 2022) found the waterbelt to be unviable, even with sea-glacier albedo as low as 0.45. Most recently, Hörner and Voigt (2023) showed that the waterbelt in earlier models resulted from inadequate vertical resolution in the sea ice.

(d) Ice surface. Vincent and Howard-Williams (2000), and Vincent et al. (2000), suggested that microbial life could survive on the ice surface of Snowball Earth, pointing to the widespread microbial communities that thrive both in surface meltwater pools and in brine pockets, on modern Arctic and Antarctic sea ice and ice shelves. These communities can persist even if only a few days per year have temperatures above freezing. Such communities could indeed have been active during the rapid advance of sea ice at the onset of Snowball Earth. But after the ice reaches the equator, the strong positive albedo-temperature feedback causes dramatic cooling. An early general circulation model (GCM) of the hard snowball by Pollard and Kasting (2004)

obtained a global average surface temperature of -49°C. The warmest temperature on the ocean surface was found on a summer afternoon in the subtropics, ~-30°C, which seemed to rule out any surface life. However, we will see below that Vincent's proposal can be resurrected if it is considered in combination with the next proposed refugium *(e).*

(e) Narrow bay. One place where ocean water could be safe from sea-glacier inflow is at the innermost end of a narrow bay resulting from continental rifting, like the modern Red Sea. When flowing into a narrow bay, nearly enclosed by dry land, ice flow can be slowed by resistive shear stresses from the side-walls, and by obstacles such as islands, shoals, or narrows in the bay. If the bay is long enough and the sublimation rate is high enough, the ice thickness can taper down to zero before the end of the bay is reached (Campbell et al., 2011, 2014). To illuminate these concepts, in the Appendix we derive a characteristic penetration distance based on a simplified sea glacier in a simplified bay, in the absence of geometric complexities. If ocean-sourced water flowing under the ice can find its way to the end of the narrow bay, it could provide a refugium safe from sea glaciers. If the surrounding land is net-evaporative (i.e., potential sublimation outpaces precipitation, as in deserts), this place would be safe from land glaciers as well.

Refugia in narrow bays would be larger than the isolated geothermal hotspots around volcanic islands, and would have long lifetimes, similar to timescales of continental drift. But even if the end of the bay is safe from sea-glacier inflow, there is the risk that the climate might still be so cold that thick sea ice would grow locally. Such a refugium would be feasible only if local temperatures reach above freezing, which could occur because the albedo of nearby bare land surfaces would be lower than that of the ice-covered ocean. Land surfaces during the Snowball Earth events were not vegetated: possible snow-free surfaces would be bare rock, bare soil, and sand. Most of them are brighter than vegetated land, but with albedos 0.1-0.4 they are

much darker than ice or snow. To evaluate the feasibility of this refugium, climate modeling is needed, and that is the subject of this paper.

2. Investigation of the ocean-bay refugium

Given the high uncertainty of Neoproteorozoic paleocontinental reconstructions, for this investigation we apply an earth-system model to the *modern* continental configuration. This approach has been used in prior investigations, called "modern Snowball Earth" (Voigt and Marotzke, 2010; Liu et al., 2018). It has the advantage of familiar geography, allowing comparisons of atmospheric circulation and climate with the familiar regional climates of the present. We take the modern continental configuration as a representative arrangement of continents of various size and shape, scattered across a range of latitudes.

As potential refugia, in addition to nearly-enclosed seas such as the Red Sea and Mediterranean, we also seek locations on land where the local temperature exceeds the freezing point of seawater at least once during the year; i.e. $T_{max} > -2°C$. With the right coastline geometry in a paleocontinental configuration (to allow for ocean-water access), these locations would be potential oases for photosynthetic eukaryotes.

Continental positioning itself is uncertain, and coastline geometry of the Neoproterozoic is even more uncertain. The period was tectonically active, and thus we make an explicit assumption that narrow bays are likely to have occurred and therefore seasonally above-freezing temperatures on land in our "modern Snowball Earth" allow for potential refugia even if these areas are not currently near a modern narrow bay. Additionally, many narrow bays would be smaller than the resolution of a typical global Earth System Model; thus, we focus on land surface temperatures as an indicator of possible refugia. To investigate whether life could survive the harshest conditions of the Snowball climate, in this paper we test the hypothesis that above-

freezing land temperatures can exist in an Earth System Model in the "hard" Snowball Earth limit, in which even the tropical oceans are covered by ice hundreds of meters thick (no waterbelt).

The name "snowball" is somewhat misleading, in that the ocean was not entirely snow-covered. On the modern Earth, evaporation (*E*) exceeds precipitation (*P*) over nearly half the ocean, mostly in the subtropics. A large region of negative *P*-*E* would also have existed on the Snowball Earth, according to general circulation models, although the hydrological cycle was probably weakened by a factor of ~30 (Pollard and Kasting, 2004). At high and middle latitudes the sea glaciers would have been covered by thick snow. But as sea glaciers flowed equatorward into the tropical region of net sublimation, their surface snow (albedo ~0.8) would sublimate away, exposing old snow ("firn", albedo ~0.7). Then the firn would likewise sublimate away, exposing bare glacier ice (albedo ~0.6) to the atmosphere and to solar radiation. These albedos were measured on modern surrogates in the Allan Hills of East Antarctica: firn and glacier ice exposed by sublimation, which have never experienced melting (Figure 1 and Table 1) (Dadic et al., 2013).

In our modeling we do not attempt to simulate the regional evolution of ocean surfaces from snow, through firn, to glacier ice, as the sea glaciers flow equatorward. Instead, everywhere that the ocean is not snow-covered, we assign its albedo to that of firn, thus biasing the global climate to a cold extreme and exaggerating the difficulty of maintaining refugia. We then investigate how the albedo of bare *land* surfaces, and the atmospheric CO_2 level, influence the potential habitability of a snowball climate. We test a range of CO_2 levels from 10 to 200 ppm and a range of uniform surface albedos for bare land from 0.2 to 0.4, using a climate model with the modern continental configuration.

During a snowball event, volcanic CO_2 accumulates in the atmosphere because its removal mechanisms (dissolving in rainwater and reacting with surface rocks) are suppressed. As the climate warmed with rising atmospheric CO_2 during the progression of a snowball event, refugia would have become more widespread. In addition, wind-erosion of bare land would have lifted dust that could accumulate on the ice, lowering its albedo, leading to additional potential mechanisms for refugia. Here we instead focus on the most extreme bottleneck of the cold early phase of a snowball event, the most critical time for survival of surface life.

3. Methods

3.1. Experimental Design

We use a modified version of the Community Earth System Model, version 2.1.0 (Danabasoglu et al., 2020), with the Simple Land Interface Model (SLIM) (Laguë et al., 2019) coupled to the Community Atmosphere Model, version 4 (CAM4) (Neale et al., 2010), the Los Alamos sea ice model CICE5 (Hunke et al., 2015) in its thermodynamic-only mode (Bitz and Lipscomb, 1999), and a slab ocean model (SOM) (Bitz et al., 2012). Ocean heat flux convergence is set to zero everywhere, and sea surface temperatures are allowed to evolve. Simulations are run at a nominal 2° resolution.

SLIM is an idealized land model, designed for assessing the interactive roles of discrete land properties (e.g. bare-ground albedo, evaporative resistance, heat capacity of the soil, etc.); using it allows us to directly assess the climate response of specified land-surface albedos. Heat diffusion in the model is represented on a vertical soil grid that is separate from the water budget. Hydrology is represented using a simple bucket model that combines a user-specified “lid” resistance with a resistance related to the fill level of the water bucket. Snow can accumulate on the surface, and can be removed by sublimation to the atmosphere or melting into the land. The

model solves a linearized surface energy budget to calculate surface temperature, surface fluxes of radiation, turbulent heat fluxes, and ground heat storage.

When snow falls on the surface of land or sea ice, it masks the albedo of the underlying surface. On land, snow masks the albedo of bare ground when it exceeds a mass of 10 kg/m^2 liquid-equivalent (about 3 to 10 cm of snow, for typical snow densities 0.1-0.3 g cm^{-3}). Land-surface models for the modern Earth normally use a larger snow-masking depth because of the presence of grass, bushes, and trees, but these plants did not appear until long after the Neoproterozoic snowball events.

In the midlatitudes and polar regions of a snowball climate, kilometer-thick ice sheets covering the oceans would accumulate, thicken, and flow like modern ice shelves towards thinner regions of net-sublimation as "sea glaciers" (Goodman and Pierrehumbert, 2003). It would therefore be glacier ice, not sea ice, that would cover the ocean surface in a snowball climate after the initial global freezing had taken place, and would have albedos ranging from that of snow in areas of snow accumulation to exposed firn and finally bare glacier ice in regions of net sublimation (Figure 1 and Table 1). Rather than predicting the detailed state of ice surface conditions, which is typical in CICE5, for simplicity we revert back to the CCSM3 shortwave radiative transfer formulation. This option allows us to prescribe "sea-ice" surface albedos. For bare (snow-free) ice we set visible and near-infrared band albedos to values appropriate for firn, so as to bias the global climate to its cold extreme. As snow accumulates, snow masks the bare ice, and the band albedos transition to values appropriate for snow (Table 1).

In all simulations, sea ice is initialized with 100% concentration and 20 m thick in all ocean gridcells. Sea ice rapidly grows thicker, but would take thousands of years to reach an equilibrium. We do not expect sea ice ever to reach an equilibrium thickness in our simulations even if we extended them, since geothermal heating is not represented; that heat source would be

necessary to limit the freezing of seawater to the base of thick ice (McKay, 2000; Warren et al., 2002; Goodman and Pierrehumbert, 2003). Our surface temperatures could be seen as too warm. For example, if the model ice thickness is only 50 m but in equilibrium would be >500 m, there is an excessive conductive heat flux of 1.4 Wm^{-2} upward through the ice, causing the surface temperature to be too high by ~0.5 K.

Over Earth's history, the Sun has brightened by about 1% every 100 million years, so at 600 Ma the solar constant was ~94% of its present value (Crowley and Baum, 1993). That value, 94%, has been used to initiate the snowball state in models with Neoproterozoic continents clustered at low latitude. The low-latitude land facilitates snowball initiation in those models, because the albedo of bare land (0.2-0.4) exceeds that of open ocean (0.07). For a “modern” Snowball Earth, with most of the continental area at middle or high latitude, a lower solar constant, about 91%, is needed to initiate the snowball (Voigt and Marotzke, 2010), and that is the value we use for this work.

In models, the critical CO_2 level required for snowball onset depends on several modeling choices: sea-ice dynamics (Lewis et al, 2006; Voigt and Abbot, 2012), land topography (Liu et al., 2018), continental configuration (Liu et al., 2013), mountains (Walsh et al., 2019), atmospheric dust (Liu et al, 2020; Liu et al., 2021), and cloud radiative forcing (Voigt and Marotzke, 2010). In prior work, modeled snowball climates have been initiated at CO_2 mixing ratios as low as 2 ppm (Voigt and Abbot, 2012) and as high as 600 ppm (Liu et al., 2017) but generally fall between 50 and 300 ppm, with exact values dependent on the ice coverage on sea and land, the solar constant, and the land area (Schrag et al., 2002; Yang et al., 2012). For the coldest early stage of a snowball event, we therefore specify a variety of CO_2 levels, along with several choices for the albedo of snow-free land, and examine the resulting climatic patterns.

For initiation of the snowball state, we set the CO_2 mixing ratio to 100 ppm, and the albedo of snow-free land to a broadband value of 0.4. The albedo of bare land (rocks or soil) increases with wavelength across the solar spectrum from the ultraviolet (UV) to the infrared (IR) (Figure 1). We specify the albedo in two bands: 0.3 in the UV and visible (wavelengths 0.3-0.7 μm), and 0.5 in the near-IR (wavelengths 0.7-5.0 μm). Under these conditions, our initial simulation establishes the conditions necessary to maintain a frozen ocean in approximately 20 years. We run the initiation simulation for a total of 100 years to ensure that the frozen-ocean state is not transient, and that the atmosphere is in steady state. Based on these conditions sufficient to generate a snowball climate, further runs are initialized with a fully ice-covered ocean to test the sensitivity of surface temperatures to variations in bare-land surface albedo and atmospheric CO_2 concentration (details below).

We run the model at the global scale and thus do not resolve the fine-scale dynamics of a sea glacier invading a bay. As described above, we assume that if a land gridcell experiences a monthly average surface temperature that exceeds the melting point, that gridcell could potentially support liquid water if a narrow arm of the sea were to reach it in a paleocontinental configuration, thus rendering it a potential refugium for photosynthetic life.

3.2. Sampling across a range of atmospheric CO_2 concentrations and land albedos

In the absence of land plants, which break up stones into sand or silt with higher albedo, the Neoproterozoic land surface was probably darker than modern deserts (the fossil record suggests that land plants did not evolve until 461–472 Ma (Kenrick et al., 2012; Morris et al., 2018)). The highest broadband albedo for modern deserts is 0.40 for the fine sand of the Arabian Empty Quarter (Smith, 1986); the lowest albedo is 0.10-0.15 for the stony desert of the western Gobi (Abell et al., 2020a; Figure S1 of Abell et al. 2020b). Within this range, we test five different sets

of snow-free land albedo values, listed here from brightest to darkest as [UV-visible albedo/near-IR albedo]: 0.3/0.5, 0.25/0.45, 0.2/0.4, 0.15/0.35, and 0.1/0.3. Approximately half the solar energy is in the near-IR, so the total solar (broadband) albedo for each case is the average of the two values given; i.e., 0.40, 0.35, 0.30, 0.25, 0.20. As a shorthand to identify the cases, we simply give the broadband values.

We sample CO_2 levels of 10, 25, 50, 100, and 200 ppm. We do not test every combination of albedo and CO_2 values, but we do test the edge cases, as well as the full range of albedos for a 50 ppm CO_2 atmosphere, and the full range of CO_2 values for land albedo 0.3 (Table 2).

We use the Parallel Offline Radiation Tool (PORT) (Conley et al., 2013) to calculate total global radiative forcing associated with each experiment relative to a base case in the middle range at CO_2 = 50 ppm and bare (snow-free) land albedo 0.3. [In Table 2 the radiative forcings are shown instead relative to the coldest case (CO_2 = 10 ppm, albedo = 0.4) for ease of comparison.] Table 2 shows that dropping the albedo of bare land from the brightest case (0.4) to the darkest case (0.2) at 50 ppm causes a radiative forcing (RF) of 4.06 W/m^2, resulting in a 5.2 K increase in global mean surface temperature, implying a climate sensitivity of 1.28 $K/(Wm^{-2})$. Increasing CO_2 from 10 ppm to 200 ppm (with land albedo 0.3) causes RF = 5.16 Wm^{-2}, and results in a temperature increase of 2.8 K, implying a lower climate sensitivity of 0.54 $K/(Wm^{-2})$. These climate sensitivities may be compared to a median of 0.5 $K/(Wm^{-2})$ in 19 GCMs for the modern Earth (Cess et al., 1990).

These climate sensitivities indicate that albedo-driven forcing kicks off stronger feedbacks than CO_2-driven forcing. The snowball climate has been shown to be relatively insensitive to CO_2-driven forcing; at such low temperatures, the positive feedback from the water-vapor greenhouse effect is weak (Pierrehumbert 2005). Outside of the tropics, the wintertime greenhouse effect is negative, resembling the modern Antarctic plateau (Sejas et al., 2018). The

greenhouse effect can be calculated as $G = \sigma T_S^4 - OLR$, where σ is the Stefan-Boltzmann constant, and OLR is outgoing longwave radiation. Surface temperature change due greenhouse warming is $\Delta T_g = T_S - [OLR/\sigma]^{1/4}$. At 50 ppm, G ranges from 0.7 W m^{-2} to 2.6 W m^{-2}, and ΔT_g, is between 0.9 and 2.3 K (higher warming at lower bare-land albedo). At 200 ppm and 0.2 albedo, G is 4.4 W m^{-2}, and ΔT_g reaches 3.5 K. Pierrehumbert (2005) obtained a similarly small value for the global average on a hard snowball; their Figure 4 shows a clear-sky greenhouse effect of ~8 W m^{-2}. These snowball values are much smaller than those for the modern Earth, where $G \approx 150$ W m^{-2} and $\Delta T_g = 33$ K.

4. Results

4.1. Some of the land surface has above-freezing mean-annual temperatures, and much more has above-freezing temperatures seasonally.

In our runs with lower bare-land albedo, we find small areas of land that are above-freezing on annual average. These areas allow for the potential of "open water" refugia. But refugia do not require open water. If the end of an oceanic bay is below freezing on annual average, but the warmest month is above freezing, sea ice would form in the bay, and it would partially melt in summer. Neoproterozoic algae could have survived in the temporary meltwater pools on the ice, as has been observed by mat-forming eukaryotic algae on the McMurdo Ice Shelf and on the Ward Hunt Ice Shelf in the Canadian Arctic (Vincent, et al., 2000; Vincent and Howard-Williams, 2000). In these modern analogs, organisms can survive perennially in ice that is deeply frozen for all but a few weeks or days per year. This would be the "ice surface" refugium described above in Section 1.1(d).

We find that in our coldest case (10 ppm CO_2, bare-land albedo 0.4), 0.1% of the land surface area reaches temperatures above the freezing temperature of seawater (-2°C) in at least

one month of the year, despite a global mean surface temperature of -69°C (Figure 2a). In our warmest case (200 ppm CO_2, bare-land albedo 0.2) in which global mean surface temperature is -61°C, 17% of land surface area reaches temperatures warm enough to host liquid water in the warmest month. (Our specification of the freezing temperature as -2°C is a conservative choice. With perhaps 20% of the ocean water converted to land glaciers and sea glaciers, the salinity of the remaining seawater would increase, lowering its freezing temperature closer to -3°C.)

To investigate how refugia might form, we calculate the potential evaporation (PE, mm/day), a measure of the rate at which the atmosphere could evaporate or sublimate water from the surface, if that surface had unlimited water availability. Over land, we calculate PE using a modified version of the Penman-Monteith equation (Penman, 1948; Monteith, 1981; Scheff and Frierson, 2014). Over the ocean, it is equal to the latent heat flux from the ocean to the atmosphere converted to units of water flux (mm/day). The dry snowball atmosphere over land creates demand for water resulting in large areas of the land surface that are snow-free for part of the year (Figure 2d-f). Above-freezing land surfaces are concentrated in places where PE outpaces precipitation – in particular, parts of the Arabian Peninsula, the modern Sahara Desert and eastern Asia (compare Figures 2a-c and 2g-i). Without snow cover, low-albedo land absorbs more solar radiation, allowing for above-freezing local land temperatures and the potential for unfrozen water and refugia if an ocean bay were to intrude to those locations.

A net-evaporative location experiencing mean-annual temperatures above freezing may thus serve as a refugium if it is connected via a narrow bay to the ocean, allowing seawater from below the sublimating sea glacier to flow into the bay and replace the water lost by evaporation.

Our model does not represent the growth of ice sheets on land. However, we can infer that snow-covered regions in Figure 2d-f are where ice sheets would grow; where they would flow would depend on the land's topography. Ice sheets have been directly simulated on

Neoproterozoic continents (Donnadieu et al., 2003; Benn et al., 2015); they cover only parts of the continents, allowing large regions to be ice-free land.

4.2. Land surface albedo exerts control on the habitability of nearly-enclosed bays.

Land surface temperatures increase more strongly in response to decreases in bare-land surface albedo than to increases in CO_2, for the same magnitude of global radiative forcing. This response occurs across all latitudes and is stronger in regions with more total land area (Figure 3a). Starting from a baseline of albedo 0.4 and 10 ppm CO_2, increasing CO_2 from 10 to 200 ppm constitutes a global radiative forcing of 5.16 Wm^{-2}, while decreasing snow-free land albedo from 0.4 to 0.2 constitutes a smaller forcing of 4.06 Wm^{-2} yet causes a greater increase of warm land area. The change of land area per unit of radiative forcing is shown in Figure 3b, for four cases of similar RF, two caused by increasing CO_2 and the others by decreasing albedo. Despite smaller globally mean radiative forcing from albedo changes, land surface temperatures are more responsive to albedo since the radiative forcing is concentrated over snow-free land.

Decreasing bare-land albedo facilitates potential refugia in two ways: (1) warming of bare land and (2) exposing new bare land that then becomes warm. In our simulations, both mechanisms occur to effect a change in habitability, with approximately 45% of the newly exposed land above freezing (in the warmest month) having become warm enough to host refugia through the first mechanism, and 55% through the second mechanism at constant CO_2. (Partitioning is similar at 10, 50, and 200 ppm CO_2). We do not see above-freezing temperatures in locations that have snow cover. If a warm, net-precipitating location did exist, it would become a warm ice sheet, like a modern temperate glacier or the wet-snow zone of modern Greenland.

Either decreasing bare-land albedo or raising CO_2 expands the area of potentially habitable land in coastal gridcells; continental interiors already meet the criteria for potential habitability at albedo 0.4. A world with low bare-land albedo would therefore be more likely to host life in narrow bays that intrude into the dark land. As mentioned above, the bare land in the Neoproterozoic probably resembled modern stony deserts rather than sand or soil, so its albedo may have been even lower than the lowest case we modeled (broadband albedo 0.2).

Figure 4 and Table 2 show, for the various combinations of CO_2 and albedo, the percent of land area capable of hosting refugia, were an arm of the sea to reach it, demonstrating again the relative importance of global radiative forcing by land albedo and CO_2. Starting from the coldest case (bare-land albedo 0.4, CO_2=10 ppm), positive radiative forcing results from either increasing CO_2 or reducing land albedo. For the same radiative forcing, a change of land albedo is more effective than a change of CO_2. Figure 4a shows this for the annual maximum temperature (T_{max}); the area of above-freezing land ranges from 0.1% to 12%, by decreasing bare-land albedo alone. [Even in the warmest case (bare-land albedo 0.2, CO_2=200 ppm), we do not see places with *annual mean* temperature $\bar{T}$>-2°C. That would allow for "open-water" refugia, because during at least part of the year the bay would be ice-free.]

A temperature criterion is not sufficient. We also need $PE>P$ so that land glaciers will not form at these locations. Figure 4b shows that the percent of land area with $PE>P$ increases slightly with darkening of the land or increasing CO_2. Combining these criteria, Figure 4c shows the percent of land area with T_{max}>-2°C and $PE>P$.

There are also some small areas of the *ocean*, all on coastlines, where the surface temperature exceeds -2°C in the warmest month, but in all cases these areas represent less than 2% of the ocean area (Table 2, Figure 4d).

With high-albedo land, the climate is so cold that very little of the land reaches above freezing even with 200 ppm CO_2, as shown in Figure 4a. But with the warmer climate for darker bare land (albedo 0.2), the above-freezing land area does become sensitive to the CO_2 level (Figure 4e).

4.3 Refugia on desert land?

Besides inhabiting the ends of narrow oceanic bays, photosynthetic eukaryotes may also have been active on unglaciated land surfaces. Reviewing "early life on land", Lenton and Daines (2017) emphasized microbial mats powered by oxygenic photosynthesis. In their words: "Initially, such mats would have been dominated by [prokaryotic] cyanobacteria. Sometime during the Proterozoic Eon (2.5-0.54 Ga) they probably gained eukaryotic algae and fungi. . . . Today a mixture of cyanobacteria, algae, fungi, lichens and nonvascular plants are found in terrestrial mats, often termed 'biological soil crusts' or 'cryptogamic cover'." Lenton and Daines cited evidence that "by the start of the Neoproterozoic (1 Ga), eukaryotes were probably present alongside cyanobacteria in terrestrial mats, but whether these were algae is unclear." The soil-crust mats occur on modern midlatitude deserts that are seasonally above freezing, as in Utah and Nevada. Similar environments may therefore have offered a habitat for mixed prokaryotic/eukaryotic life in the deserts of Snowball Earth wherever the soil temperatures were above freezing seasonally, as also proposed by Retallack (2023). The locations would have to be in deserts ($PE>P$) to avoid burial by land-glaciers, but they could have received water from the local sparse precipitation, or from runoff modulated through topography.

5. Discussion and conclusion

In our simulations we used the albedo of firn rather than glacier ice (Table 1) to represent the snow-free parts of the frozen ocean, biasing the climate colder. Actual sea glaciers should have had a slightly darker surface, allowing for a warmer climate. Yet, despite our conservative choice of a brighter ice surface, our results suggest that a "hard" snowball climate with ice extending to the equator could have allowed some locations to sustain the surface liquid water needed to host photosynthetic life, despite extremely cold global-mean temperatures. Our global annual mean surface temperatures $\bar{T}$ are considerably colder than those of other GCMs simulating the hard-snowball climate. Abbot et al. (2013) reviewed six GCMs; we can estimate $\bar{T}$ from their Figure 1a for 100 ppm CO_2: for five GCMs, $\bar{T} \approx$ -38°C; the cold outlier (the FOAM GCM) had $\bar{T} \approx$ -46°C. Our finding of above-freezing locations even with our extremely cold global mean surface temperatures, all in the range -61 to -69°C (Table 1), thus argues strongly for refugia on or near ocean bays.

Although we find strong evidence to support the potential for refugia, the distribution and type of refugia (ice-surface or open-water) would be sensitive to the actual bare-land albedo. The albedo of bare land surfaces during the Neoproterozoic may have been even darker than our darkest case (albedo 0.2), as land plants had not yet evolved, which would limit the erosion of rocks into smaller grain sizes, so that stony deserts, which have broadband albedo 0.10-0.15, would be more likely than modern deserts of soil or sand. If Neoproterozoic land surfaces were indeed dark like stony deserts, this lower land albedo would result in more refugia than we have simulated here.

We find that modern nearly-enclosed bays, resulting from continental rifting (e.g. the Red Sea), are especially habitable and could support seasonal refugia depending on the land surface albedo. Since the dynamics of sea-glacier invasions into nearly-enclosed bays occur below the resolution of the model simulations employed here (Campbell et al., 2011, 2014), our

results quantify the maximum potential for refugia within a hard-snowball climate with modern continents; but the exact distribution of such nearly-enclosed bays on Neoproterozoic continents would determine true habitability. A constriction at the entrance to the bay helps to slow the sea glacier (Campbell et al., 2014), but the entrance must not be too shallow because ocean water needs a path below the ice to reach the refugium. The strait at the entrance to the Red Sea (Bab el Mandeb) is only 137 m deep (Siddall et al., 2002), so a sea glacier would likely become grounded there.

Since Neoproterozoic continental reconstructions are constrained primarily by paleomagnetism, which constrains the latitude but not the longitude, there remains large uncertainty in the likelihood of large continental interiors, which we expect to strongly influence our results (Merdith et al., 2021). The total land area was probably only slightly smaller than today's (Hawkesworth et al., 2019), but the tropical bias in land distribution and degree of continental "clumping", as well as the location and height of mountain ranges, could influence our results (Laguë et al., 2023).

Our conclusion is that the ends of narrow oceanic bays were likely to serve as refugia for photosynthetic eukaryotes, even during the coldest early phase of a snowball event.

Acknowledgments.

This work was supported by NSF grant AGS-20-41491, and by a grant of time on NCAR computers. MML acknowledges funding from the James S. McDonnell Foundation Postdoctoral Fellowship in Dynamic and Multiscale Systems (grant # 220020576). We acknowledge helpful discussions with Ursula Jongebloed, Bonnie Light, and Tyler Kukla. Figure 1 was drafted by Richard Brandt.

Data availability statement.

Model results are available through the University of Washington Libraries Dryad repository (https://datadryad.org/stash/share/gpuwaesE07cQpgj_PwzewJaQdOLBSANcDtdSF_aK6hc). Source code for CESM and SLIM, the models used in this study, are archived and publicly accessible online (https://doi.org/10.5281/zenodo.3895306), with development code publicly available on GitHub (https://escomp.github.io/CESM/release-cesm2/downloading_cesm.html) for CESM.

Conflict of Interest Statement.

The authors have no conflicts of interest to declare.

Appendix. *Penetration of a sea glacier down a narrow bay.*

A sea glacier entering a long narrow bay with length L_{bay} could be expected to have some spatial and temporal variability in flow speed and thickness, due for example to obstructions such as islands, shoals, or narrows in the bay; however, we can look beyond those possibly minor variations to find characteristic numbers describing important aspects of long, straight, narrow bays, their sea glaciers, and their climates.

We use a coordinate system [*x*,*y*,*z*], with *x* and *y* horizontal; *x* can be aligned along the axis of the bay, with *x*=0 at the bay mouth, and *z* is vertical. The corresponding velocity components are [*u*,*v*,*w*].

If a bay has a roughly uniform width *W*, then flow *v*(*x*,*y*) transverse to the long axis of the bay is small.

A sea glacier is floating, so except on shoals, there is no basal friction, and the flow speed *u*(*x*,*y*,*z*) along the bay can be treated as independent of depth, i.e. as *u*(*x*,*y*).

Nye (1965) found a solution appropriate for *u*(*x*,*y*) for floating ice in a uniform deep narrow channel or deep bay, and Campbell et al. (2011) averaged Nye's solution across the bay to find its average value $\bar{u}(x)$,

$$\bar{u}(x) = \frac{W}{2}\,\frac{A(x)k(x)^n}{n+2}. \qquad (1)$$

Temperature (and therefore ice softness) is incorporated in *A*(*x*), resistive side-wall drag is incorporated in *k*(*x*), and $n \cong 3$ is the exponent in the Glen nonlinear flow law for ice (Glen, 1955).

Thomas (1973), and Sanderson (1979) showed that $\bar{u}(x)$ varies little in *x*, so following Campbell et al. (2011) we set $\bar{u}$ to be a constant, which we take as a characteristic velocity u_{char}.

Ablation rate *b*(*x*) (m/s) depends on sublimation on the upper surface and melting at the base; however, Goodman (2006) found that in the tropics on Snowball Earth, basal melting was insignificant relative to surface sublimation. Although sublimation rate can vary along a long

narrow bay, following Campbell et al. (2011), we can define a characteristic ablation rate b_{char} as the average value of $b(x)$ along the centerline of the bay (b<0 for sublimation).

A characteristic ice thickness H_{char} is set by the offshore sea glacier, which enters the bay and moves from its mouth at x=0 to the glacier terminus at x=L_{glac} where the ice thickness reaches zero. Time t_{flow} for ice to travel the distance L_{glac} is inversely proportional to the speed u_{char}; t_{flow} is also the time needed to sublimate the full ice thickness H_{char} at rate -b_{char}. Equating these two time estimates,

$$t_{flow} = \frac{L_{glac}}{u_{char}} = \frac{H_{char}}{-b_{char}} . \quad \text{(A2)}$$

Solving Eq. (A2) for the penetration length L_{glac} in terms of the characteristic values,

$$L_{term} = - (H_{char}\, u_{char}) / b_{char} . \quad \text{(A3)}$$

Eq. (A3) shows that penetration length L_{glac} is shorter when u_{char} is smaller (e.g. due to obstructions that impede ice flow along the bay), and when sublimation rate b_{char} is larger in magnitude (e.g. due to a warmer drier climate of the surrounding desert). Thickness H_{char} of the sea glacier on the adjacent ocean also matters; however, H_{char} is controlled by external factors beyond the narrow bay.

A characteristic steady-state thickness profile $h(x)$ can also be found. The volumetric flux $q(x)$ (m^3/s) is volume of incompressible ice passing through a "gate" across the bay with area W $h(x)$ at each position x, given by

$$q(x) = u_{char} W\, h(x), \quad \text{(A4)}$$

and the mass-conservation equation takes the form

$$dq/dx = W\, b_{char} . \quad \text{(A5)}$$

Putting Eq. (A4) into (A5) gives

$$dh/dx = b_{char} / u_{char} . \quad \text{(A6)}$$

Integrating Eq. (A6) with the boundary condition $h(0) = H_{char}$ yields a linear thickness profile

$$h(x) = H_{char} + (b_{char} / u_{char})\ x\ , \qquad \text{(A7)}$$

and the sea glacier terminates where h=0, i.e. at L_{term} given in Eq. (A3) above.

Examples with greater spatial variability, fewer assumptions, and additional physical details will be more complicated (e.g. see Campbell et al. (2011; 2014)); however, this simple analytical solution can provide insights to guide refinements and approximations.

The existence of a refugium at the end of the bay requires $L_{glac} < L_{bay}$.

References

Abbot, D.S., Voigt, A., & Koll, D. (2011). The Jormungand global climate state and implications for Neoproterozoic glaciations. *Journal of Geophysical Research: Atmospheres, 116*(D18), D18103.

Abbot, D.S., Voigt, A., Li, D., Le Hir, G., Pierrehumbert, R.T., Branson, M., et al. (2013). Robust elements of Snowball Earth atmospheric circulation and oases for life. *Journal of Geophysical Research: Atmospheres, 118*(12), 6017-6027.

Abell, J.T., Pullen, A., Lebo, Z., Kapp, P., Gloege, L., Metcalf, A., et al. (2020a). A wind-albedo-wind feedback driven by landscape evolution. *Nature Communications*. https://doi.org/10.1038/s41467-019-13661-w

Abell, J.T., Rahimi, S.R., Pullen, A., Lebo, Z.J., Zhang, D., Kapp, P., et al. (2020b). A quantitative model-based assessment of stony desert landscape evolution in the Hami Basin, China: Implications for Plio-Pleistocene dust production in Eastern Asia," *Geophysical Research Letters, 47*(20), e2020GL090064.

Benn, D.I., Le Hir, G., Bao, H., Donnadieu, Y., Dumas, C., Fleming, E.J., et al. (2015). Orbitally forced ice sheet fluctuations during the Marinoan Snowball Earth glaciation. *Nature Geoscience, 8*(9), 704-707.

Bitz, C.M., & Lipscomb, W.H. (1999). An energy-conserving thermodynamic model of sea ice. *Journal of Geophysical Research: Oceans, 104*(C7), 15669-15677.

Bitz, C.M., Shell, K.M., Gent, P.R., Bailey, D.A., Danabasoglu, G., Armour, K.C., et al. (2012). Climate Sensitivity in the Community Climate System Model Version 4, *J. Climate, 25*, 3053-3070, doi:10.1175/JCLI-D-11-00290.1

Bøggild, C.E., Brandt, R.E., Brown, K.J., & Warren, S.G. (2010). The ablation zone in northeast Greenland: ice types, albedos and impurities. *Journal of Glaciology, 56*(195), 101-113.

Braun, C., Hörner, J., Voigt, A., & Pinto, J.G. (2022). Ice-free tropical waterbelt for Snowball Earth events questioned by uncertain clouds. *Nature Geoscience, 15*(6), 489-493.

Budyko, M.I. (1969). The effect of solar radiation variations on the climate of the Earth. *Tellus, 21*, 611–619.

Campbell, A.J., Waddington, E.D., & Warren, S.G. (2011). Refugium for surface life on Snowball Earth in a nearly-enclosed sea? A first simple model for sea-glacier invasion. *Geophysical Research Letters, 38*(19), L19502. doi:10.1029/2011GL048846.

Campbell, A.J., Waddington, E.D., & Warren, S.G. (2014). Refugium for surface life on Snowball Earth in a nearly-enclosed sea? A numerical solution for sea-glacier invasion through a narrow strait. *J. Geophys. Res., 119*, 2679-2690, doi:10.1002/2013JC009703.

Cess, R.D., Potter, G.L., Blanchet, J.P., Boer, G.J., Del Genio, A.D., Déqué, M., et al. (1990). Intercomparison and interpretation of climate feedback processes in 19 atmospheric general circulation models. *Journal of Geophysical Research: Atmospheres, 95*(D10), 16601-16615.

Conley, A.J., Lamarque, J.-F., Vitt, F., Collins, W.D., & Kiehl, J. (2013). PORT, a CESM tool for the diagnosis of radiative forcing. *Geoscientific Model Development, 6*(2), 469-476. https://doi.org/10.5194/gmd-6-469-2013

Crowley, T.J., & Baum, S.K. (1993). Effect of decreased solar luminosity on late Precambrian ice extent. *Journal of Geophysical Research: Atmospheres, 98*(D9), 16723-16732.

Dadic, R., Mullen, P.C., Schneebeli, M., Brandt, R.E., & Warren, S.G. (2013). Effects of bubbles, cracks, and volcanic tephra on the spectral albedo of bare ice near the Transantarctic Mountains: Implications for sea glaciers on Snowball Earth. *Journal of Geophysical Research: Earth Surface, 118*(3), 1658-1676.

Danabasoglu, G., Lamarque, J.-F., Bacmeister, J., Bailey, D., DuVivier, A., Edwards, J., et al. (2020). The community earth system model version 2 (CESM2). *Journal of Advances in Modeling Earth Systems, 12*(2), e2019MS001916. https://doi.org/10.1029/2019MS001916

Donnadieu, Y., Fluteau, F., Ramstein, G., Ritz, C., & Besse, J. (2003). Is there a conflict between the Neoproterozoic glacial deposits and the snowball Earth interpretation: an improved understanding with numerical modeling. *Earth and Planetary Science Letters, 208*(1), 101-112.

Evans, D.A.D. (2000). Stratigraphic, geochronological, and paleomagnetic constraints upon the Neoproterozoic climatic paradox. *American Journal of Science, 300*(5), 347-433.

Glen, J. (1955), The creep of polycrystalline ice, *Proc. R. Soc. A*, 228, 519–538.

Goodman, J.C. (2006). Through thick and thin: Marine and meteoric ice in a "Snowball Earth" climate. *Geophysical Research Letters, 33*, L16701. doi:10.1029/2006GL026840

Goodman, J.C., & Pierrehumbert, R.T. (2003). Glacial flow of floating marine ice in "Snowball Earth". *J. Geophys. Res. Oceans, 108*(C10), 3308. https://doi.org/10.1029/2002JC001471

Grenfell, T.C., Warren, S.G., and Mullen, P.C. (1994). Reflection of solar radiation by the Antarctic snow surface at ultraviolet, visible, and near-infrared wavelengths. *J. Geophys. Res.*, **99**, 18669-18684.

Harland, W.B. (1964). Critical evidence for a great infra-Cambrian glaciation. *Geologische Rundschau, 54*(1), 45-61.

Hawkesworth, C., Cawood, P.A., & Dhuime, B. (2019). Rates of generation and growth of the continental crust. *Geoscience Frontiers, 10*, 165-173.

Hörner, J., & Voigt, A. (2023). Sea-ice thermodynamics can determine waterbelt scenarios for Snowball Earth. *EGUSphere*, doi:10.5194/egusphere-2023-2073.

Hoffman, P.F., & Schrag, D.P. (2000). Snowball Earth. *Scientific American, 68*(1), 68-75.

Hoffman, P.F., & Schrag, D.P. (2002). The Snowball Earth hypothesis: Testing the limits of global change. *Terra Nova, 14*, 129-155.

Hoffman, P.F., Abbot, D.S., Ashkenazy, Y., Benn, D.I., Brocks, J.J., Cohen, P.A., et al. (2017). Snowball Earth climate dynamics and Cryogenian geology-geobiology. *Science Advances, 3*(11), e1600983. doi: 10.1126/sciadv.1600983

Hudson, S.R., Warren, S.G., Brandt, R.E., Grenfell, T.C., & Six, D. (2006). Spectral bidirectional reflectance of Antarctic snow: Measurements and parameterization. *Journal of Geophysical Research: Atmospheres, 111*, D18106. https://doi.org/10.1029/2006JD007290

Hunke, E., Lipscomb, W.H., Turner, A., Jeffery, N., & Elliott, S. (2015). *CICE: the Los Alamos Sea Ice Model documentation and software user's manual LA-CC-06-012*. Los Alamos National Laboratory, Los Alamos, New Mexico.

Kenrick, P., Wellman, C.H., Schneider, H., & Edgecombe, G.D. (2012). A timeline for terrestrialization: consequences for the carbon cycle in the Palaeozoic. *Phil. Trans. Royal Soc. London, B367*(1588), 519–536.

Kirschvink, J.L. (1992) Late Proterozoic low-latitude global glaciation: the Snowball Earth, in *The Proterozoic Biosphere*, Schopf, J.W., and Klein, C. eds., pp. 51-52, Cambridge Univ. Press, New York.

Knoll, A.H. (2011). The Multiple Origins of Complex Multicellularity. *Annual Review of Earth and Planetary Sciences, 39*(1), 217-239.

Knoll, A.H. (2014). Paleobiological perspectives on early eukaryotic evolution. *Cold Spring Harbor Perspectives in Biology, 6*(1), a016121.

Laguë, M.M., Bonan, G.B., & Swann, A.L.S. (2019). Separating the impact of individual land surface properties on the terrestrial surface energy budget in both the coupled and uncoupled land–atmosphere system. *Journal of Climate, 32*(18), 5725-5744.

Laguë, M.M., Quetin, G.R., Ragen, S., & Boos, W.R. (2023). Continental configuration controls the base-state water vapor greenhouse effect: lessons from half-land, half-water planets. *Climate Dynamics*, https://doi.org/10.1007/s00382-023-06857-w

Lenton, T.M., & Daines, S.J. (2017). Matworld – the biogeochemical effects of early life on land. *New Phytologist, 215*, 531-537, doi:10.1111/nph.14338.

Lewis, J.P., Weaver, A.J., & Eby, M. (2006). Deglaciating the snowball Earth: Sensitivity to surface albedo. *Geophysical Research Letters, 33*(23), L23604. doi:10.1029/2006GL027774

Li, D., & Pierrehumbert, R.T. (2011). Sea glacier flow and dust transport on Snowball Earth. *Geophysical Research Letters, 38*(17), L17501.

Liu, Y., Peltier, W.R., Yang, J., & Vettoretti, G. (2013). The initiation of Neoproterozoic "snowball" climates in CCSM3: the influence of paleocontinental configuration. *Climate of the Past, 9*(6), 2555-2577.

Liu, Y., Peltier, W.R., Yang, J., Vettoretti, G., & Wang, Y. (2017). Strong effects of tropical ice-sheet coverage and thickness on the hard snowball Earth bifurcation point. *Climate Dynamics, 48*(11), 3459-3474.

Liu, Y., Peltier, W.R., Yang, J., and Hu, Y. (2018). Influence of surface topography on the critical carbon dioxide level required for the formation of a modern Snowball Earth. *Journal of Climate, 31*(20), 8463-8479.

Liu, P., Liu, Y., Peng, Y., Lamarque, J.-F., Wang, M., & Hu, Y. (2020). Large influence of dust on the Precambrian climate. *Nature Communications, 11*(1) 4427.

Liu, Y., Liu, P., Li, D., Peng, Y., & Hu, Y. (2021). Influence of dust on the initiation of Neoproterozoic Snowball Earth events. *Journal of Climate, 34*(16) 6673-6689.

Macdonald, F.A., Schmitz, M.D., Crowley, J.L., Roots, C.F., Jones, D.S., Maloof, A.C., et al. (2010). Calibrating the Cryogenian. *Science, 327*(5970), 1241-1243.

McKay, C.P. (2000). Thickness of tropical ice and photosynthesis on a snowball Earth. *Geophysical Research Letters, 27*(14), 2153-2156.

Merdith, A.S., Williams, S.E., Collins, A.S., Tetley, M.G., Mulder, J.A., Blades, M.L., et al. (2021). Extending full-plate tectonic models into deep time: Linking the Neoproterozoic and the Phanerozoic. *Earth-Science Reviews, 214*, 103477.

Monteith, J.L. (1981). Evaporation and surface temperature. *Quart. J. Roy. Meteor. Soc, 107*, 1-27.

Morris, J.L., Puttick, M.N., Clark, J.W., Edwards, D., Kenrick, P., Pressel, S., et al. (2018). The timescale of early land plant evolution. *Proc. Nat. Acad. Sci. USA, 115* (10), E2274-E2283. doi:10.1073/pnas.1719588115.

Neale, R.B., Richter, J.H., Conley, A.J., Park, S., Lauritzen, P.H., Gettelman, A. Williamson, D.L., et al. (2010). *Description of the NCAR Community Atmosphere Model (CAM 4.0)* (NCAR/Tn-485+Str), National Center for Atmospheric Research, Boulder, Colorado.

Nye, J. F. (1965), The flow of a glacier in a channel of rectangular, elliptical or parabolic cross-section, *J. Glaciol.*, 5, 661–690.

Penman, H.L. (1948). Natural evaporation from open water, bare soil and grass. *Proc. Roy. Soc. London, 193A*, 120-145.

Pierrehumbert, R. T. (2005). Climate dynamics of a hard snowball Earth. *J. Geophys. Res. Atmos., 110*, D01111, doi:10.1029/2004JD005162.

Pollard, D., & Kasting, J.F. (2004) Climate-ice sheet simulations of Neoproterozoic glaciation before and after collapse to Snowball Earth, in *The Extreme Proterozoic: Geology, Geochemistry, and Climate, Geophys. Monogr. Ser.*, vol. 146, edited by G. Jenkins et al., pp 91-105, AGU, Washington, D.C.

Pollard, D., & Kasting, J.F. (2005). Snowball Earth: A thin-ice solution with flowing sea glaciers. *J. Geophys. Res., 110*, C07010, doi:10.1029/2004JC002525.
Pollard, D., Kasting, J.F. & Zugger, M.E. (2017). Snowball Earth: Asynchronous coupling of sea-glacier flow with a global climate model. *J. Geophys. Res. Atmos., 122*, 5157-5171, doi:10.1002/2017JD026621.
Porter, S.M. (2004). The fossil record of early eukaryotic diversification. *The Paleontological Society Papers, 10*, 35–50.
Retallack, G.J. (2023). Neoproterozoic Snowball Earth extent inferred from paleosols in California. *J. Palaeosciences, 72,* 9-28, doi:10.54991/jop.2023.1851.
Sanderson, T. J. O. (1979), Equilibrium profile of ice shelves, *J. Glaciol*., 22, 435–460.
Scheff, J., & Frierson, D.M.W. (2014). Scaling potential evapotranspiration with greenhouse warming. *Journal of Climate, 27*(4), 1539-1558.
Schrag, D.P., Berner, R.A., Hoffman, P.F., & Halverson, G.P. (2002). On the initiation of a snowball Earth. *Geochemistry, Geophysics, Geosystems, 3*(6) 1-21. https://doi.org/10.1029/2001GC000219
Sellers, W.D. (1969). A global climatic model based on the energy balance of the earth-atmosphere system. *Journal of Applied Meteorology and Climatology, 8*(3), 392-400.
Sejas, S.A., Taylor, P.C. & Cai, M. (2018). Unmasking the negative greenhouse effect over the Antarctic Plateau. *npj Clim Atmos Sci 1*, 17.
Siddall, M., Smeed, D., Matthiesen, S., & Rohling, E. (2002). Modelling the seasonal cycle of the exchange flow in Bab el Mandab (Red Sea). *Deep Sea Research Part I, 49*(9), 1551-1569.
Smith, E.A. (1986). The structure of the Arabian heat low. Part I: Surface energy budget. *Monthly Weather Review,114*(6), 1067-1083.
Thomas, R. H. (1973), The creep of ice shelves: Theory, *J. Glaciol*., 12, 45–53.
Vincent, W.F, & Howard-Williams, C. (2000). Life on Snowball Earth. *Science, 287*(5462), 2421-2421.
Vincent, W.F., Gibson, J.A.E., Pienitz, R., Villeneuve, V., Broady, P.A., Hamilton, P.B., & Howard-Williams, C. (2000). Ice Shelf Microbial Ecosystems in the High Arctic and Implications for Life on Snowball Earth. *Naturwissenschaften, 87*(3), 137-141.
Voigt, A., & Abbot, D.S. (2012). Sea-ice dynamics strongly promote Snowball Earth initiation and destabilize tropical sea-ice margins. *Climate of the Past, 8*(6), 2079-2092.
Voigt, A., & Marotzke, J. (2010). The transition from the present-day climate to a modern Snowball Earth. *Climate Dynamics, 35*(5), 887-905.
Voigt, A., Abbot, D.S., Pierrehumbert, R.T., & Marotzke, J. (2011). Initiation of a Marinoan Snowball Earth in a state-of-the-art atmosphere-ocean general circulation model. *Climate of the Past, 7*(1), 249-263.
Walsh, A., Ball, T., & Schultz, D.M. (2019). Extreme sensitivity in Snowball Earth formation to mountains on PaleoProterozoic supercontinents. *Scientific Reports, 9*(1), 2349.
Warren, S.G., & Brandt, R.E. (2006). Comment on "Snowball Earth: A thin-ice solution with flowing sea glaciers" by David Pollard and James F. Kasting. *Journal of Geophysical Research, 111*, C09016.
Warren, S.G., Brandt, R.E., Grenfell, T.C., & McKay, C.P. (2002). Snowball Earth: Ice thickness on the tropical ocean. *J. Geophys. Res., 107*(C10), 3167.
Yang, J., Peltier, W.R., & Hu, Y. (2012). The initiation of modern soft and hard Snowball Earth climates in CCSM4. *Climate of the Past, 8*(3) 907-918.

Tables

Table 1. Band-albedos of representative snow, ice, and land surfaces. The spectral albedos for four of these surface types are shown in Figure 1.

Surface type	Albedo			
	0.3-0.7 μm (UV, visible)	0.7-3.0 μm (near-infrared)	0.3-3.0 μm (total solar; broadband)	Reference
Snow	0.98	0.68	0.83	Hudson et al. (2006), Grenfell et al. (1994)
Firn	0.94	0.44	0.69	Dadic et al. (2013)
Glacier ice	0.89	0.26	0.58	Dadic et al. (2013)
Polar desert (gravel and soil of northeast Greenland)	0.13	0.21	0.17	Bøggild et al. (2010)
Sand desert (Arabia)			0.40	Smith (1986)
Stony desert (Gobi)			0.10-0.15	Abell (2020ab)

Table 2. Characteristics of the model runs. The consequences of radiative forcing shown for combinations of changes to the bare-land albedo and the CO_2 level are relative to the coldest case of CO_2 = 10 ppm and bare-land albedo = 0.4 broadband (0.3 visible / 0.5 near-IR). Land is "net-evaporative" if potential evaporation (PE) exceeds precipitation (P).

Albedo of bare (snow-free) land		CO_2 (ppm)	Global average planetary albedo	Global mean surface temperature (°C)	Radiative forcing (W m^{-2}) relative to 10 ppm, albedo 0.4	Percent of land area with T_{max} > -2°C in warmest month	Percent of land area with $PE>P$ in annual mean	Percent of land area with $PE>P$ and T_{max} > -2°C	Percent of ocean area with T_{max}>-2°C in warmest month
Broadband solar	Visible/near-IR								
0.4	0.3/0.5	10	0.683	-69.2	0	0.1	50.8	0.1	0
0.4	0.3/0.5	50	0.681	-67.9	2.75	0.23	54.16	0.23	0.01
0.4	0.3/0.5	200	0.68	-66.5	5.16	0.54	59.83	0.54	0.04
0.35	0.25/0.45	50	0.675	-66.6	3.78	1.41	57.67	1.41	0.11
0.3	0.2/0.4	10	0.67	-66.7	2.05	3.1	56.77	3.1	0.24
0.3	0.2/0.4	25	0.669	-66.0	3.6	3.48	59.9	3.45	0.31
0.3	0.2/0.4	50	0.668	-65.3	4.8	4.04	63.14	4.04	0.36
0.3	0.2/0.4	100	0.667	-64.6	5.99	5.27	66.32	5.27	0.49
0.3	0.2/0.4	200	0.667	-63.9	7.21	5.72	70.4	5.7	0.40
0.25	0.15/0.35	50	0.662	-64.0	5.81	9.15	68.16	9.02	0.87
0.2	0.1/0.3	10	0.657	-64.2	4.06	12.15	67.87	12.02	1.17
0.2	0.1/0.3	50	0.655	-62.7	6.81	14.99	74.57	14.82	1.53
0.2	0.1/0.3	200	0.653	-61.2	9.22	17.22	85.03	17.05	1.83

743 ***Figures***

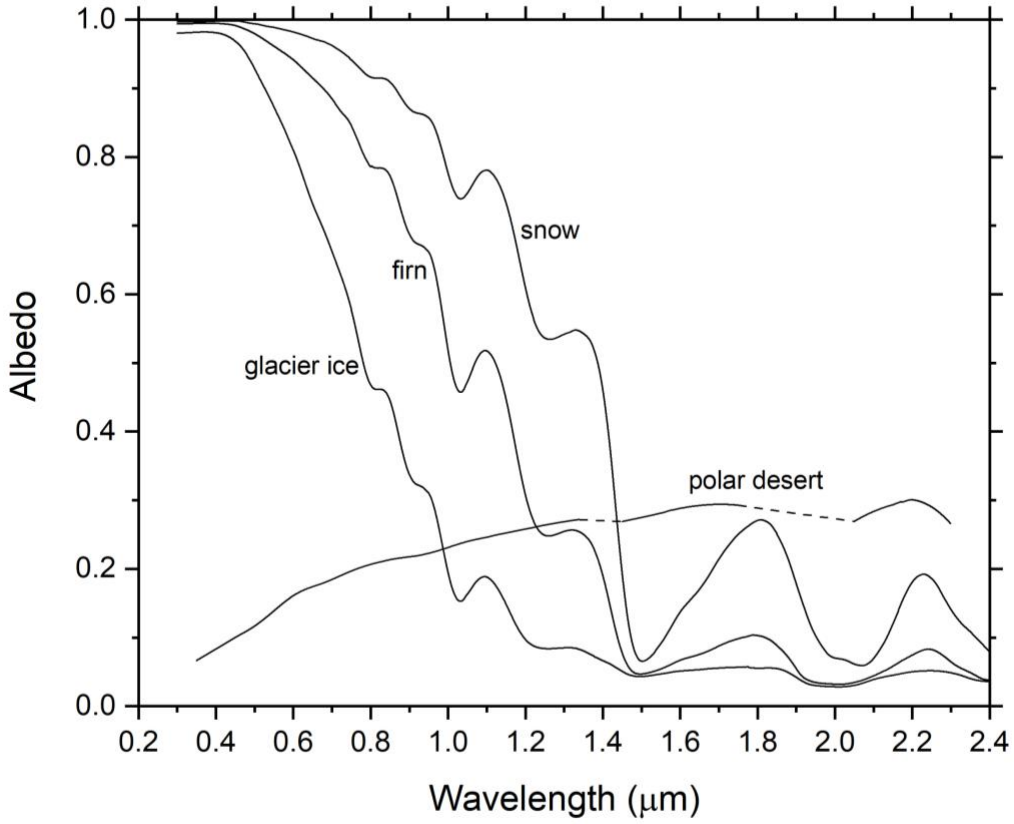

744

745 **Figure 1.** Spectral albedos of representative surface types. Cold fine-grained snow was measured
746 at Dome C on the East Antarctic Plateau (Figure 6 of Hudson et al., 2006). Firn was measured
747 just upstream of the Allan Hills blue-ice field in East Antarctica (Site R9 of Dadic et al., 2013).
748 Glacier ice is from the Allan Hills blue-ice field (Site R1 of Dadic et al., 2013). These firn and
749 ice sites can represent sea-glacier surfaces on Snowball Earth because they were originally
750 formed by snow accumulation and exposed by sublimation, never having experienced melting.
751 The "polar desert" site is an unvegetated surface of soil and stones in northeast Greenland
752 (photograph shown in Figure 6 of Bøggild et al., 2010). For the “polar desert” surface, albedo
753 measurements were not possible from 1.35 to 1.45 μm, and from 1.75 to 2.05 μm, because the
754 incident solar radiation flux was near zero at these wavelengths due to atmospheric water-vapor
755 absorption; the dashed lines interpolate across these regions.

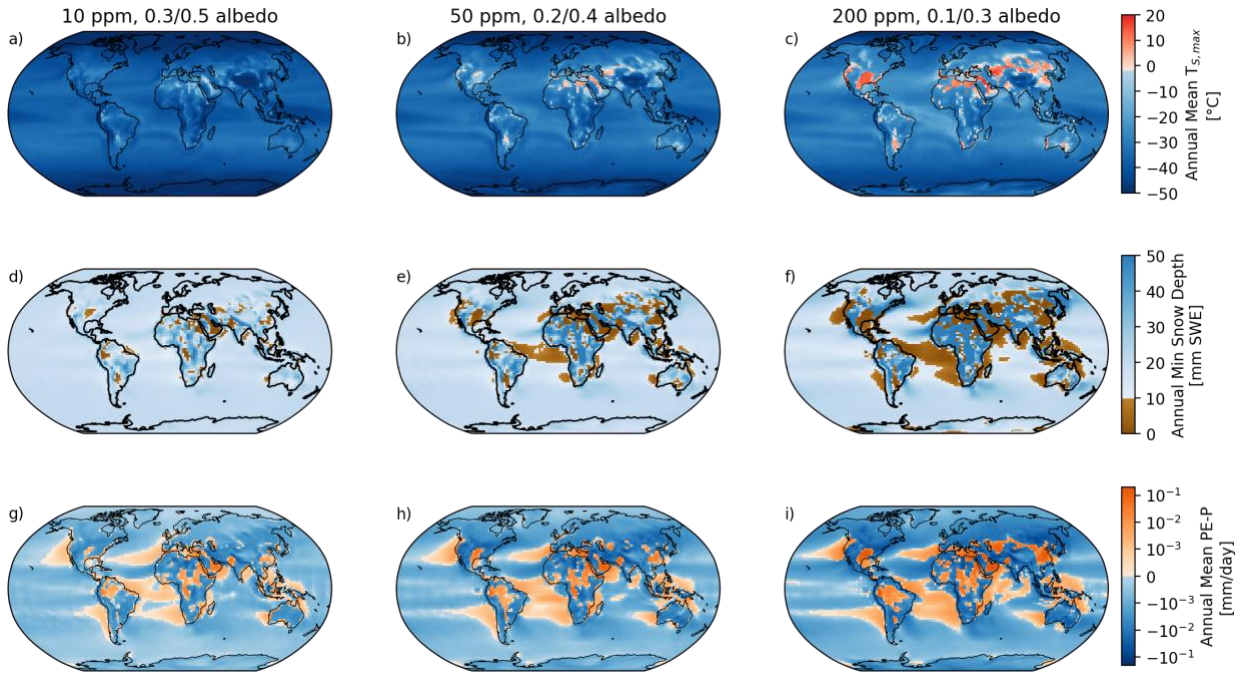

Figure 2. Habitability of the simulated snowball climate. **(a, b, c)** Surface temperature of the warmest month in the coldest simulated case (10 ppm CO_2, bare-land albedo 0.4), the midpoint simulation (50 ppm CO_2, bare-land albedo 0.3) and the warmest case (200 ppm CO2, bare-land albedo 0.1), respectively. Red areas indicate locations with seasonal melting, suggesting the possiblity of ice-surface refugia. (**d, e, f)** Annual minimum snow depth (monthly mean) from the same cases, given as mm snow water equivalent (SWE), which is equivalent to kg/m^2. Brown areas indicate places where snow depth drops below the threshold for surface-albedo change at some point during the year. Note that ocean areas without snow accumulation would nonetheless be covered by sea glaciers. (**g, h, i)** Annual mean potential evaporation (PE) minus precipitation (P) for the same cases.

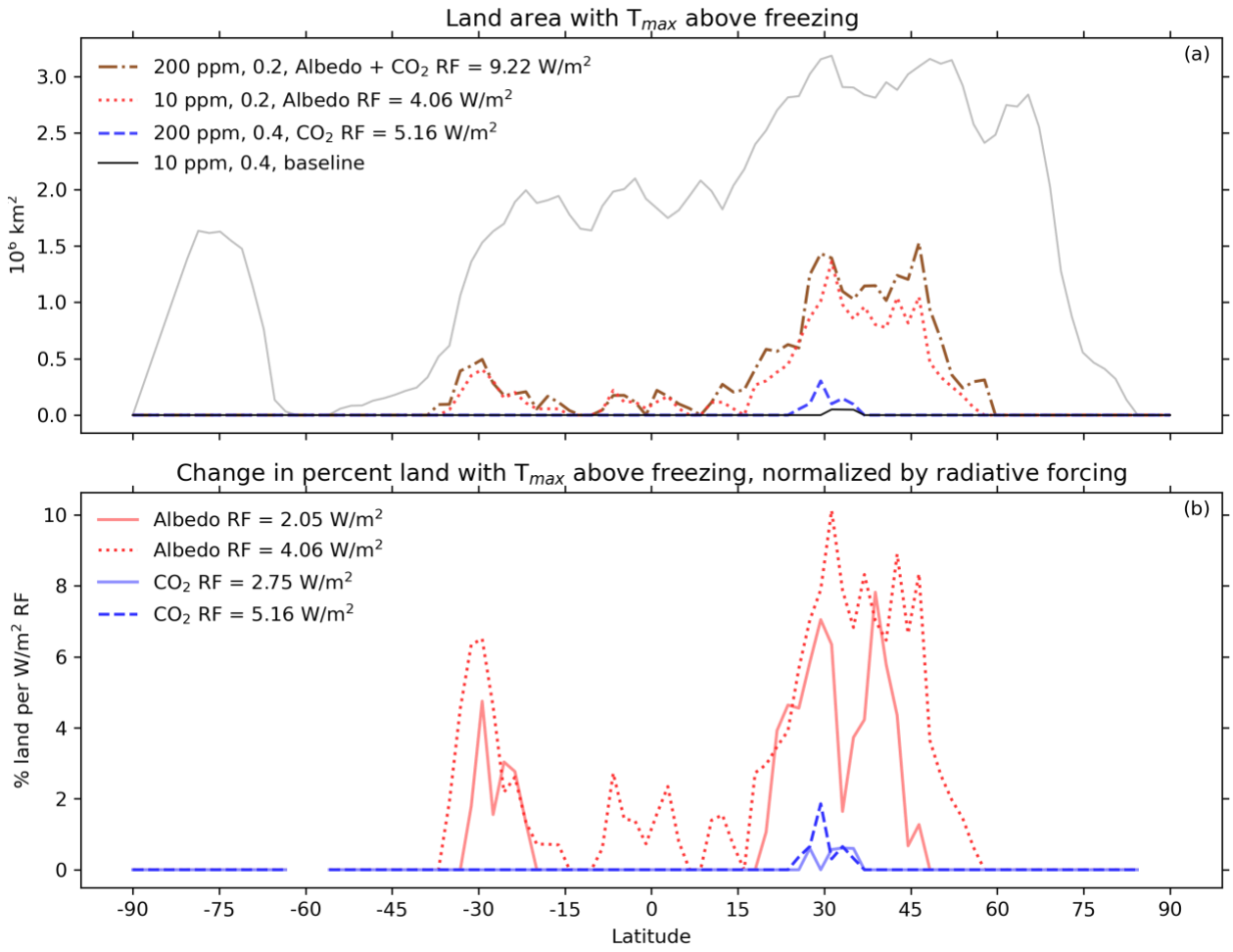

Figure 3. **(a)** Area of land (per 1.9 degrees of latitude increment) with temperature above freezing in the warmest month. Total land area is shown in grey. **(b)** Change in percent land area above freezing in the warmest month, per unit radiative forcing, relative to the coldest case (10 ppm CO_2, albedo 0.4).

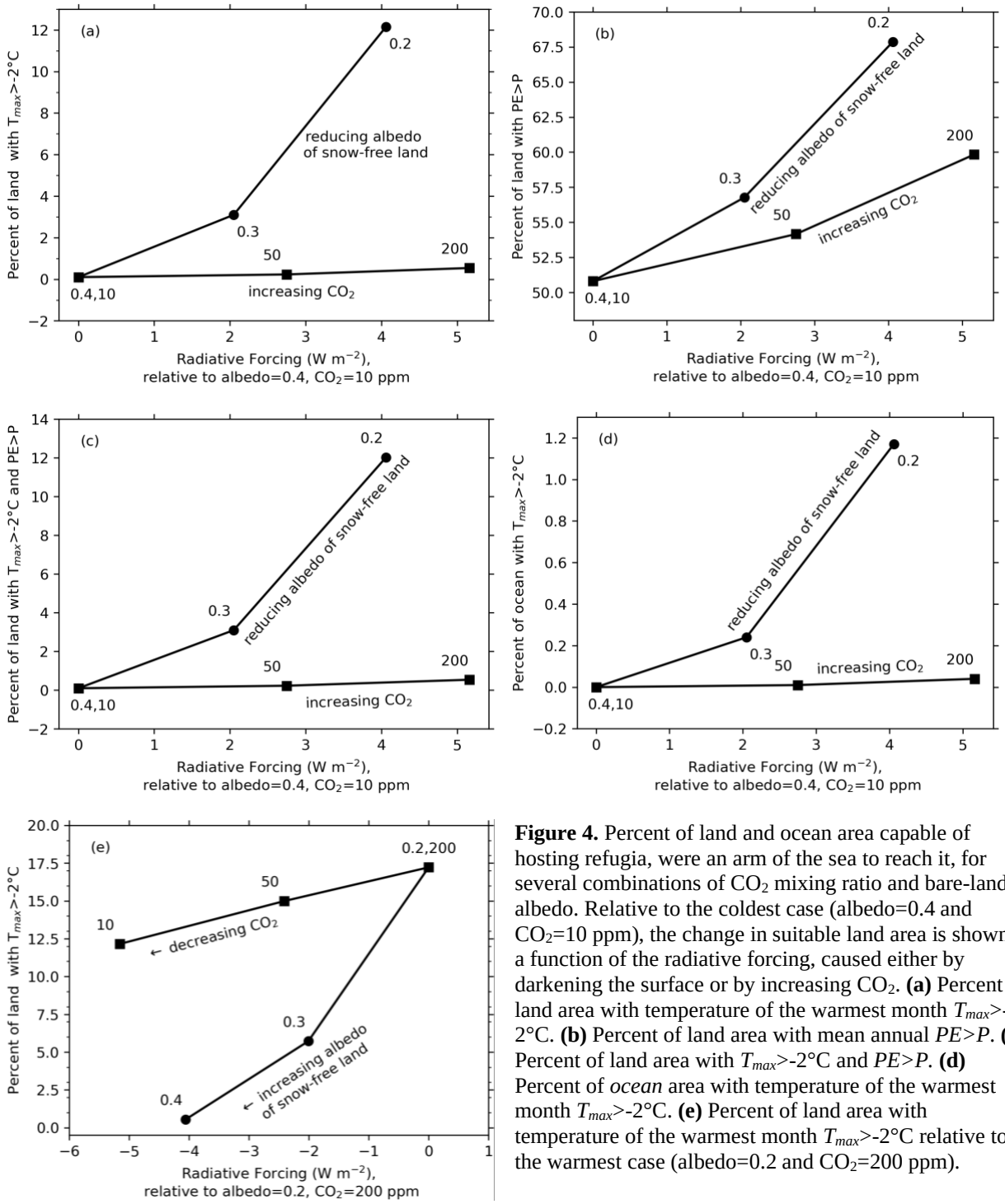

Figure 4. Percent of land and ocean area capable of hosting refugia, were an arm of the sea to reach it, for several combinations of CO_2 mixing ratio and bare-land albedo. Relative to the coldest case (albedo=0.4 and CO_2=10 ppm), the change in suitable land area is shown as a function of the radiative forcing, caused either by darkening the surface or by increasing CO_2. **(a)** Percent of land area with temperature of the warmest month T_{max}>-2°C. **(b)** Percent of land area with mean annual $PE>P$. **(c)** Percent of land area with T_{max}>-2°C and $PE>P$. **(d)** Percent of *ocean* area with temperature of the warmest month T_{max}>-2°C. **(e)** Percent of land area with temperature of the warmest month T_{max}>-2°C relative to the warmest case (albedo=0.2 and CO_2=200 ppm).